Journal of Applied Polymer Science

Ethanol organosolv lignin as a reactive filler for acrylamide-based hydrogels

Bai-Liang Xue,[1] Jia-Long Wen,[1] Run-Cang Sun[1,2]

[1]Beijing Key Laboratory of Lignocellulosic Chemistry, Beijing Forestry University, Beijing 100083, China

[2]State Key Laboratory of Pulp and Paper Engineering, South China University of Technology, Guangzhou 510640, China

Correspondence to: R.-C. Sun (E-mail: rcsun3@bjfu.edu.cn)

ABSTRACT: Hydrogels based on acrylamide (AM) and ethanol organosolv lignin (EOL) with high swelling and good mechanically elastic properties were synthesized in an alkaline solution. EOL was used as a reactive filler for the preparation of AM-based hydrogels. The impact of EOL addition on the physicochemical properties of AM-based hydrogels was investigated using Fourier transform infrared (FTIR) spectroscopy and scanning electron microscopy, and their mechanical properties were examined. The water swelling ratio of the prepared hydrogels increased with the increase of EOL content, and their maximum swelling ratio could reach up to 180. Mechanical measurements indicated that their tensile strength was highly dependent on the amount of EOL, and their elongation at break reached up to 1400%. The formation mechanism of EOL composite hydrogels was probably that most of AM was synthesized into the crosslinked poly(acrylic amide) network, and small quantities of AM was hydrolyzed to acrylic acid ions under alkaline condition. The chain transfer of free radicals from AM and/or AA to EOL molecules occurred in the polymerization process. With increasing EOL content in the hydrogels, an interpenetrating polymer network might be mainly formed by the hydrogen bonding between EOL and AA and/or AM molecules. © 2015 Wiley Periodicals, Inc. J. Appl. Polym. Sci. **2015**, *132*, 42638.

KEYWORDS: biomaterials; gels; mechanical properties; morphology

Received 11 September 2014; accepted 17 June 2015

DOI: 10.1002/app.42638

INTRODUCTION

Hydrogels are natural or synthetic crosslinked polymeric materials that can absorb large amounts of water while remaining insoluble in aqueous solutions because of chemical or physical crosslinking of individual polymer chains.[1–9] The hydrogels made from natural polymers could offer several advantageous properties such as inherent biocompatibility and biodegradability. The emerging technologies of hydrogels helped to improve many fields ranging from food industry and cosmetics to pharmaceuticals and biomedical implants.[10] However, these hydrogels could not provide sufficient mechanical properties.

Lignin, a natural phenolic polymer in higher plant tissues, is a major component in wood constituting roughly 15–35% by weight.[11] It is a three-dimensional amorphous polymer arising from *p*-coumaryl alcohol, coniferyl alcohol, and/or sinapyl alcohol.[12] In the secondary cell walls of vascular plants, lignin fills the spaces between cellulose and hemicelluloses, providing mechanical strength to the lignocellulose matrix.[13] Lignin also binds fibers together to form a strong and tough matrix of plants and provides mechanical support to the plant vessels for the transportation of water and nutrients.[14] To date, enormous amounts of lignin polymer are primarily produced as waste products in papermaking industry and burnt as a fuel in the pulping process. Because of their complex structure and less accessible reactivity of hydroxyl groups, limited lignin products (~ 2%) focused primarily on low-value products such as stabilizers, dispersants, and surfactants.[15,16] Hence, the great challenge in lignin utilization is to find novel and highly value-added applications of lignin.

Several approaches for the preparation of water-swelling lignin or its derivatives based on hydrogels have previously been proposed by researchers in the last decade, for example, chemical crosslinking of kraft lignin, alkali lignin, acetic acid lignin, or water-soluble lignosulfonates with epichlorhydrin, formaldehyde, glutaraldehyde, or polyethylene glycol diglycidyl ether.[17–20] Other attempts involved graft copolymers from kraft lignin, alkaline lignin, or acetic acid lignin with *N*-isopropylacrylamide, poly(vinyl alcohol), and acrylamide (AM).[21–24] Moreover, interpenetrating polymer network (IPN) could be formed in the network of kraft lignin/starch/AM-based hydrogels.[25] However, the raw material used in these studies is industrial lignin, which contains less chemical reactivity due to the harsh chemical pulping process. Ethanol organosolv process, as an environmentally

friendly technology, uses aqueous ethanol to extract lignin from lignocelluloses in the presence of small amount of inorganic acid as a catalyst.[26,27] Ethanol organosolv lignin (EOL) has attractive potential properties in developing high-value lignin products, such as higher purity, less condensed structure, higher hydroxyl content, narrower molecular weight distribution, and plausibly higher reactivity than lignosulfonates and alkali lignins.[28] In addition, the impact of EOL addition on the physicochemical properties of AM-based hydrogels has not yet been investigated.

In this study, a new type of AM-based hydrogels was synthesized with EOL used as a reactive filler in the presence of *N*,*N*-methylene-bis-acrylamide (MBA) as the crosslinker and ammonium persulfate (APS) as the initiator. The effect of EOL content on the swelling behavior, interior morphology, and mechanical property of the prepared hydrogels was fully investigated. The possible formation mechanism of EOL composite hydrogels was proposed.

EXPERIMENTAL

Materials

Birch wood (*Betula alnoides*) was collected from Yunnan Province (Southern China) and milled into wood meal (20–40 mesh). AM, APS, and MBA was used as the monomer, initiator, and crosslinker, respectively. All the chemical reagents were of analytical grade and obtained from Beijing Chemical Reagent Factory, China, and used without further purification.

Extraction of EOL

EOL was prepared by the ethanol organosolv pulping procedure according to the literature with a slight modification.[29] In brief, 5 g of Birch wood meal was treated with a 60% ethanol solution with a solid to liquid ratio of 1 : 10 (g/mL) at 200°C for 1.5 h under nitrogen atmosphere using a 1.0-L stainless steel reactor (Parr). After treatment, the reactor was rapidly cooled down, the pulp was filtrated, and washed repeatedly by 60% ethanol solution. Then, the filtrates (∼ 100 mL) were concentrated to about 20 mL under reduced pressure. Subsequently, the concentrated liquor was poured into three volumes of water to precipitate the lignin. After stirring vigorously, the separation of the precipitated lignin will then be achieved in a filter washer. Finally, the lignin obtained was freeze-dried prior to use.

Preparation of Hydrogels

A single factor was used to optimize the synthetic conditions of AM-based hydrogels by adjusting the crosslinker content based on the literature with a slight modification.[25,30] First, 2.0 g of AM and 20.0 mL deionized water were completely mixed with 10 wt % NaOH solution added dropwise maintaining pH at 11. Different amounts of MBA (70, 80, 90, 100, and 110 mg) were then poured into the aqueous solution under constant stirring until the mixtures were homogeneously dissolved. Finally, 10 mg of APS was added into the above solution at constant stirring, and the resulting solution in polytetrafluoroethylene molds was allowed to proceed in a vacuum oven at 65°C for 3 h under nitrogen atmosphere until the hydrogels were formed. The purified hydrogels were obtained by immersing the hydrogels into excess distilled water for 24 h to remove any NaOH fractions. The effect of crosslinker addition on the water swelling ratio of AM-based hydrogels is summarized in Table I.

Table I. Effect of Addition of Crosslinker Content on Water Swelling Ratio of AM-Based Hydrogels

Crosslinker (mg)	Initiator (mg)	AM (g)	Swelling ratio
70	10	2	48
80	10	2	61
90	10	2	76
100	10	2	82
110	10	2	69

For the preparation of EOL composite hydrogels, these hydrogels were prepared at 65°C by free radical polymerization of AM and EOL in an alkaline solution using APS as an initiator. Various amounts of EOL (10, 20, and 30 mg) were added into the alkaline solution (pH 11) prior to the addition of 100 mg MBA and 10 mg APS. With the exception of EOL, the procedure was the same for the preparation of AM-based hydrogels. For all the synthesis, the amount of EOL varied, whereas AM, MBA, and APS compositions were maintained as listed in Table II. The purified hydrogels obtained with 0, 10, 20, and 30 mg of EOL were abbreviated as LH0, LH1, LH2, and LH3, respectively. All the samples were prepared by the same procedure mentioned above, except for the amounts of EOL. For mechanical measurements, the purified hydrogels were dehydrated to constant weight at room temperature until their polymer/water weight ratio was kept constant. The dry hydrogels were used for swelling ratios and Fourier transform infrared (FTIR) spectra measurement by drying the purified hydrogels under vacuum at 75°C for 48 h. In the morphological measurement, the swollen hydrogels were prepared by immersing the dry hydrogels into the excess water at 25°C for 24 h.

Characterization of Hydrogels

Water swelling ratios of the dry hydrogels were measured as follows: dried cubic samples ($1 \times 1 \times 1$ cm^3) were weighted and immersed into the excess water without any stress at 25°C, and then, the sample was taken out at certain time intervals, surface water was removed with filter paper, and the weight of the wet hydrogel was determined gravimetrically.

The water swelling ratio was calculated according to the following equation:

$$\text{Swelling ratio} = (W_s - W_d) \times 100 / W_d \quad (1)$$

where W_s is the weight of the wet hydrogel and W_d is the weight of the dry hydrogel. Three water swelling ratio experiments were conducted for each sample to ensure reproducibility.

FTIR spectra were recorded using a Thermo Scientific Nicolet iN10 FTIR Microscope (Thermo Nicolet Corporation, Madison, WI) equipped with a liquid nitrogen-cooled MCT detector. The spectra were measured from 4000 to 650 cm^{-1} (spectral resolution: 4 cm^{-1}; 128 scans per spectrum). The dry hydrogels were

Table II. Composition of EOL Composite Hydrogels

Code	EOL (mg)	AM (g)	MBA (mg)	10% NaOH[a] (mL)	APS (mg)
LH0	0	2	100	20	10
LH1	10	2	100	20	10
LH2	20	2	100	20	10
LH3	30	2	100	20	10

[a] 10% NaOH was defined as the 10 wt % NaOH solution.

frozen in liquid nitrogen and then ground to a fine powder using a mortar and pestle before measurement.

In the morphological study, the swollen hydrogels were frozen at −50°C and then vacuum-dried at −50°C for 24 h (Thermo Fisher). The freeze-dried hydrogels were fractured carefully in liquid nitrogen. The internal faces of the fragments obtained were coated by a sputter-coating (BOT 341F) with evaporated gold (in 4 nm thickness), and subsequently, its morphology was examined using a scanning electron microscopy (SEM; Hitachi 3400N) at an acceleration voltage of 15 kV.

Mechanical properties were evaluated using Zwick Z005 testing machine at room temperature (25°C ± 1°C). The measurement conditions were shown as follows: crosshead speed = 30 mm/min, gauge length = 20 mm, and hydrogel size 5 mm × 40 mm × 8 mm. To minimize dehydration, a thin layer of low viscosity of silicone oil was coated on the sample surface. The tensile strength and elongation at break were recorded, and the modulus was calculated from the increase in load detected from an elongation of 50–150%. For each sample, five parallel experiments were conducted to ensure good reproducibility (±5%).[29]

RESULTS AND DISCUSSION

Synthesis of EOL Composite Hydrogels

To select the optimized condition for producing higher swelling ratio of AM-based hydrogels, a single factor was used to optimize their synthetic conditions by changing the crosslinker content. Table I shows that the crosslinker addition has obvious effect on their water swelling ratio. The sample has the highest swelling ratio (82) when the addition of crosslinker content was 100 mg. When the crosslinker content added was lower than 100 mg, their water swelling ratio increased gradually with the increase of MBA concentration. In contrast, when the addition of crosslinker content was higher than 100 mg, their water swelling ratios started to decline. This is related to the fact that the crosslinker density affects the water swelling process. When the crosslinker density was lower than the optimum value (100 mg/20 mL), the monomer could not be adequately grafted. As a result, the process of the chain transfer reaction was restricted, and the growth of grafting polymer chains was affected. Then, the three-dimensional network could not be efficiently formed. Thus, the water swelling ratio increased with the increase of MBA below the optimal value. However, a higher crosslinker density usually produced more crosslink points, and thus, the network space left for holding water was gradually reduced. As a result, the increase of crosslinker density above the optimum value led to the decrease of the water swelling ratio. Furthermore, to enhance their good mechanically elastic property, different amounts of EOL were incorporated into the AM-based hydrogels. The photographs of the hydrogels with different amounts of EOL are shown in Figure 1, and it was clear that their color were gradually deepened from colorless to dark brown with the increase of EOL. The amount of EOL was a critical parameter in the formation of EOL composite hydrogels and had a strong influence on their physicochemical properties, that is, appearance, mechanical properties, water absorption, and retention capacity.

FTIR of EOL Composite Hydrogels

FTIR spectroscopy is a highly effective analytical tool to study the interactions between different polymers. As shown in Figure 2, the characteristic bands of the functional groups were shown as follows: N—H stretching (3550–3340 cm^{-1}), C—H stretching (2950–2850 cm^{-1}), amide I band or C=O stretching (1668 cm^{-1}), amide II band or C—N stretching, and N—H bending vibration (1565 cm^{-1}).[31] The crosslinked poly(acrylic amide) (PAM) exhibited distinct peaks at 3358 and 3189 cm^{-1}, representing N—H asymmetric and symmetric stretching. The peaks at 1668 and 1565 cm^{-1} correspond to the C=O stretching of the amide I band and C—N stretching, respectively. These absorptions indicated that the PAM existed in all the samples. The absorption peaks at 1565 and 1447 cm^{-1} are probably related to the asymmetric and symmetric stretching of the carboxylate anion, respectively.[32] These results indicated partial hydrolysis of the amide group into a carboxylate group and production of the acrylic acid ions through partial hydrolysis reaction.[33,34] The hydrolysis was further confirmed by the appearance of another sharp peak at 1408 cm^{-1}, which is ascribed to the symmetric stretching mode of the carboxylate

Figure 1. Representative photographs of hydrogels with different EOL content (LH0, LH1, LH2, and LH3). [Color figure can be viewed in the online issue, which is available at wileyonlinelibrary.com.]

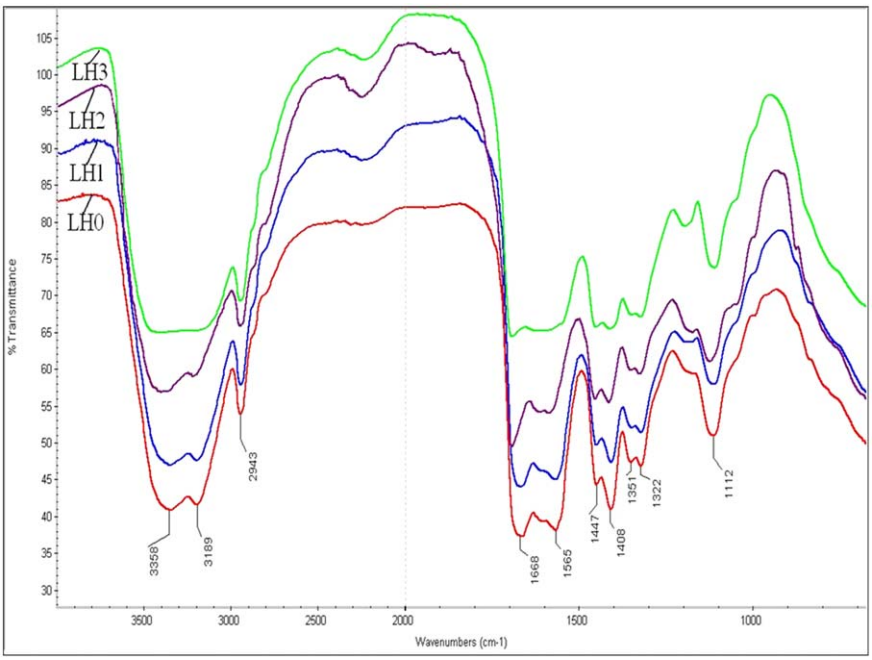

Figure 2. FTIR spectra of hydrogels with different EOL content (LH0, LH1, LH2, and LH3). [Color figure can be viewed in the online issue, which is available at wileyonlinelibrary.com.]

anion.[35,36] The copolymerization of EOL with AM and/or AA occurred in the polymerization process, resulting from the chain transfer of free radicals to EOL molecules. However, when compared with the samples LH0 and LH1, the peak for C═O stretching vibration was shifted to higher region (1700 cm^{-1}) in the samples LH2 and LH3. These results suggested that the hydrogen bonding of the EOL with AA and/or AM molecules mainly enhanced with increasing EOL content. Furthermore, it should be noted that the intensity in the peak of 1408 cm^{-1} decreased with the increase of EOL content. The reduced

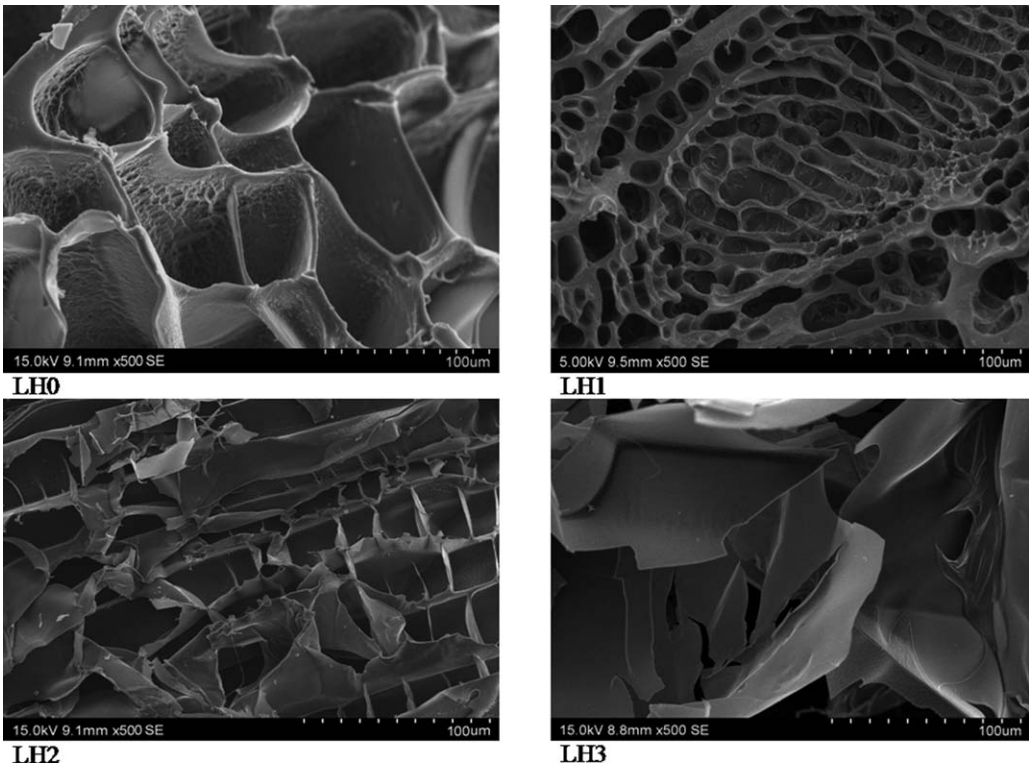

Figure 3. SEM micrographs of internal morphology of hydrogels with different EOL content (LH0, LH1, LH2, and LH3).

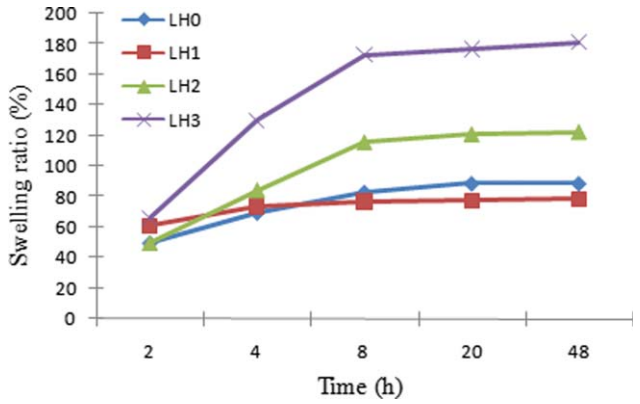

Figure 4. Water swelling behaviors of hydrogels with different EOL content as a function of time (LH0, LH1, LH2, and LH3). [Color figure can be viewed in the online issue, which is available at wileyonlinelibrary.com.]

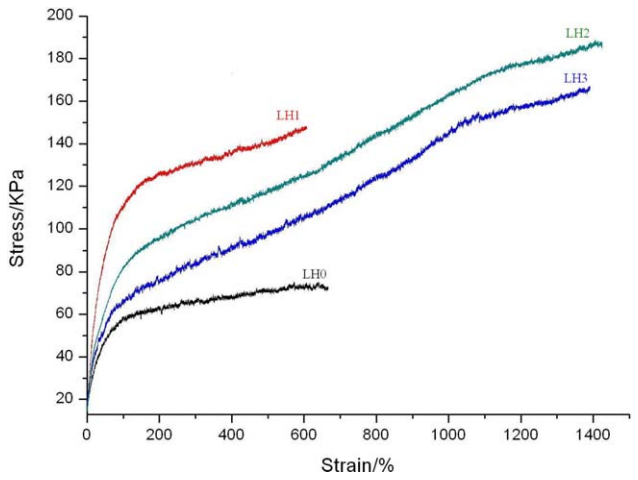

Figure 5. Stress–strain curves of hydrogels with different EOL content (LH0, LH1, LH2, and LH3). [Color figure can be viewed in the online issue, which is available at wileyonlinelibrary.com.]

intensity is probably due to more free radicals transferred to EOL molecules with increasing EOL content, resulting in more EOL precipitating in the graft copolymerization reaction. Additionally, the bands around 1600–1400 cm^{-1} assigned to the aromatic skeletal vibrations of lignin were weak. In contrast, the band at 2943 cm^{-1} associated with the stretching vibrations of methylene groups was still remarkable, suggesting that the AM and/or AA molecules were probably grafted onto the aromatic ring of EOL.[37]

Morphology of EOL Composite Hydrogels

The morphological characteristics of the samples were observed by SEM to establish the presence of possible interactions between different components. As shown in Figure 3, the micrograph of the control sample LH0 showed a homogenous morphology with continuous honeycomb-like structures, which were mainly due to the formation of the crosslinked PAM network. However, it is unexpected that the pores of the sample LH1 were smaller than those of the sample LH0, leading to the finding that the sample LH1 had denser structure than the sample LH0. In the smaller microporous network of the sample LH1, EOL was used as a chemically crosslinked polymer, which is attributable to the graft copolymerization reaction between the EOL and AM and/or AA. With the increasing EOL content in the AM-based hydrogels, the hydrogen bonding between the EOL and AM and/or AA was mainly increased instead of their crosslinked linkages, and the sheet-like structure in the surface of the samples LH2 and LH3 was partially or fully formed by lignin, which supports the discussion in the section of FTIR analysis. In fact, the lignin is an interpenetrated phase dispersed in the synthetic matrix, forming an IPN, which is in agreement with a previous publication.[38] This kind of porous structure results in an increased surface area and capillary effect, which are related to the water absorbency and retention rate of EOL composite hydrogels.[32]

Water Absorption of EOL Composite Hydrogels

Water swelling ratio is a very important parameter because it represents the amount of water retention within the hydrogel network. The water swelling ratios of all the samples are shown in Figure 4. It is clear that the EOL addition had obvious effect on the water swelling ratios of AM-based hydrogels. When the samples were used to measure the water absorption process, their water swelling ratios increased with increasing swelling time. Their maximum water swelling ratios increased from 70 to 180 when the amounts of EOL increased from 10 to 30 mg in the prepared hydrogels. In comparison with the samples LH0 and LH1, the higher swelling ratios of the samples LH2 and LH3 were probably due to the abundant polar groups (aromatic and aliphatic hydroxyls, carbonyls, and ethers) of lignin. In the sample LH1, by involving itself in the graft copolymerization reaction, the hydroxyl groups of EOL moieties were blocked by forming ether linkages in the network. However, with the increase of EOL addition in the samples LH2 and LH3, their

Table III. Composition of Raw Materials, Conditions for Hydrogel Synthesis, and Tensile Properties of Hydrogels

	Synthesis		Tensile test		
Hydrogel samples	EOL[a] (mg)	Reaction time (h)	Tensile strength (kPa)	Elongation (%)	Modulus (kPa)
LH0	0	3	72.57 ± 1.7	666.46 ± 5.3	12.51 ± 1.8
LH1	10	3	148.25 ± 5.4	607.33 ± 2.6	32.63 ± 2.9
LH2	20	3	187.41 ± 2.5	1406.68 ± 3.5	27.87 ± 5.3
LH3	30	3	167.42 ± 1.7	1389.16 ± 6.7	18.91 ± 2.4

[a] EOL (ethanol organosolv lignin), monomer (AM, 2 g), crosslinker (MBA, 100 mg), and initiator (APS, 10 mg) were added into 20 mL deionized water.

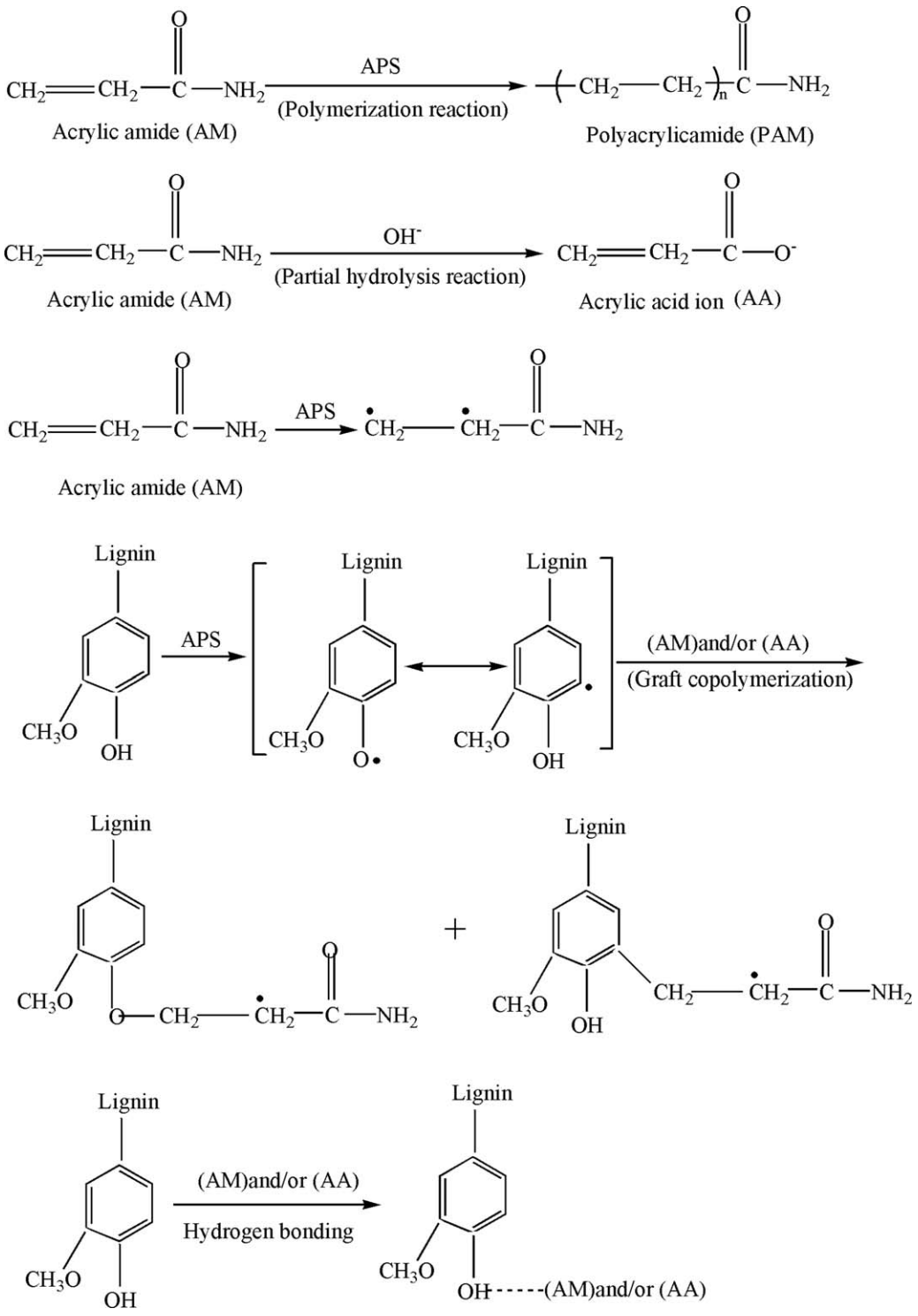

Figure 6. Suggested reaction mechanism for the formation of EOL composite hydrogels.

hydrogen-bonding interactions mainly existed between polymer chains and water in the three-dimensional matrix, which led to a more relaxed network with higher swelling capacity.[39] Additionally, it is interesting to note that the sample LH1 exhibited a slight lower water swelling ratio than that of the control sample LH0, which was probably attributed to the fact that the sample LH1 had denser structure than that of the control sample LH0 based on the analysis of SEM.

Mechanical Properties of EOL Composite Hydrogels

The stress–strain curves of the samples are shown in Figure 5, and the average values of tensile strength, modulus, and

elongation ratio are summarized in Table III. At a given monomer concentration, different amounts of EOL were added into the AM-based hydrogels, which showed excellent mechanical flexibility, such as elongation at break.

When compared with the modulus of the control sample LH0 (12.51 kPa), the modulus of the sample LH1 increased sharply to 32.63 kPa. However, the modulus decreased regularly with increasing EOL content. The modulus of 27.87 kPa corresponded to the sample LH2 and 18.91 kPa to the sample LH3. With respect to their mechanical behaviors during the tensile process, EOL composite hydrogels showed higher tensile strength than those of the control sample, and their tensile strength were highly dependent on EOL content. The tensile strength increased from 72.57 kPa for the control sample LH0 to 148.25 kPa for the sample LH1, further increased to 187.41 kPa for the sample LH2, and finally slightly dropped to 167.42 kPa for the sample LH3. Furthermore, the elongation at break of the samples LH0 and LH1 was 666.46 and 607.33%, respectively. In contrast, the elongation at break of the samples LH2 and LH3 was almost 1400%. These results suggested that small amounts of EOL addition (20–30 mg) could greatly enhance their elongation at break. With response to the interesting phenomenon of the elongation at break, some points should be addressed. On one hand, the relative poor elongation at break ratio of the samples LH0 and LH1 was originated from a randomly crosslinked network that led to a wide distribution of polymer chain length, and a lack of an efficient energy dissipation system in the network that resulted in low resistance to crack propagation.[30] On the other hand, the samples LH2 and LH3 could be viewed as near elastic under the high deformation, and the IPN might be mainly formed by the hydrogen bonding when excess amounts of EOL were used as a dispersed phase, which significantly dissipated the crack energy along the polymer chains and prevented crack propagation.[40]

Based on the above results, the presumed reaction mechanism for the formation of EOL composite hydrogels was proposed as shown in Figure 6. In the synthesis of EOL composite hydrogels, most of the AM was synthesized into the crosslinked PAM network, and a small amount of AM was converted into the acrylic acid ions through partial hydrolysis reaction under the alkaline condition. The graft copolymerization of EOL with AM and/or AA occurred in the polymerization process, resulting in the chain transfer of free radicals to EOL molecules. With increasing EOL content in the AM-based hydrogels, an IPN might be mainly formed by the hydrogen bonding between EOL and AA and/or AM molecules.

CONCLUSIONS

Excellent mechanically elastic EOL composite hydrogels with a high water absorption swelling based on lignin were successfully developed via the crosslinked copolymer network, with MBA as the crosslinker and APS as the initiator. The water absorption capacity of the hydrogels increased with increasing EOL content. The tensile modulus of the hydrogels containing EOL was higher than that from the free EOL composite hydrogels, but it decreased regularly with the increase of EOL content. The elongation at break of the prepared hydrogels reached up to 1400% with a certain amount of EOL. In short, the excellent properties, such as high water absorption, high tensile modulus, and excellent elongation at break, will lead to EOL composite hydrogels, which are promising materials for water retention applications.

ACKNOWLEDGMENTS

This work was supported by the State Forestry Administration (grant number: 201204803), the National Natural Science Foundation of China (grant numbers: 31110103902 and 31430092), and the Fundamental Research Funds for the Central Universities (grant number: BLYJ201312).

REFERENCES

1. Vermonden, T.; Censi, R.; Hennink, W. E. *Chem. Rev.* **2012**, *112*, 2853.
2. Wang, Q. G.; Mynar, J. L.; Yoshida, M.; Lee, E.; Lee, M.; Okuro, K.; Kinbara, K.; Aida, T. *Nature* **2010**, *463*, 339.
3. Wang, J. F.; Lin, L.; Cheng, Q. F.; Jiang, L. *Angew. Chem. Int. Ed. Engl.* **2012**, *51*, 4676.
4. Huang, T.; Xu, H.; Jiao, K.; Zhu, L.; Brown, H. R.; Wang, H. *Adv. Mater.* **2007**, *19*, 1622.
5. Akagi, Y.; Katashima, T.; Katsumoto, Y.; Fujii, K.; Matsunaga, T.; Chung, U. I.; Shibayama, M.; Sakai, T. *Macromolecules* **2011**, *44*, 5817.
6. Cheng, Q. F.; Wu, M. X.; Li, M. Z.; Jiang, L.; Tang, Z. Y. *Angew. Chem. Int. Ed. Engl.* **2013**, *52*, 3750.
7. Cheng, Q. F.; Li, M. Z.; Tang, Z. Y. *Adv. Mater.* **2012**, *24*, 1838.
8. Cheng, Q. F.; Jiang, L.; Tang, Z. Y. *Acc. Chem. Res.* **2014**, *47*, 1256.
9. Wang, J. F.; Cheng, Q. F.; Tang, Z. Y. *Chem. Soc. Rev.* **2012**, *41*, 1111.
10. Lin, C. C.; Metters, A. T. *Adv. Drug Deliv. Rev.* **2006**, *58*, 1379.
11. Pushpamalar, V.; Langford, S. J.; Ahmad, M.; Lim, Y. Y. *Carbohydr. Polym.* **2006**, *64*, 312.
12. Borges da Silva, E. A.; Zabkova, M.; Araujo, J. D.; Cateto, C. A.; Barreiro, M. F.; Belgacem, M. N.; Rodrigues, A. E. *Chem. Eng. Res. Des.* **2009**, *87*, 1276.
13. Ritter, S. K. *Chem. Eng. News* **2008**, *86*, 15.
14. Pan, X. J.; Saddler, J. N. *Biotechnol. Biofuels* **2013**, *6*, 12.
15. Dohertya, W. O. S.; Mousavioun, P.; Fellows, C. M. *Ind. Crop. Prod.* **2011**, *33*, 259.
16. Stewart, D. *Ind. Crop. Prod.* **2008**, *27*, 202.
17. Lindström, T.; Westmen, L. *Colloid Polym. Sci.* **1980**, *258*, 390.
18. Yamamoto, H.; Amaike, M.; Saitoh, H.; Sano, Y. *Mater. Sci. Eng. C* **2000**, *7*, 143.
19. Nishida, M.; Uraki, Y.; Sano, Y. *Bioresour. Technol.* **2003**, *88*, 81.

20. Passauer, L.; Fischer, K.; Liebner, F. *Holzforschung* **2011**, *65*, 309.
21. El-Zawawy, W. K. *Polym. Adv. Technol.* **2005**, *16*, 48.
22. Kim, Y. S.; Kadla, J. F. *Biomacromolecules* **2010**, *11*, 981.
23. Feng, Q. H.; Chen, F. G.; Wu, H. R. *Bioresources* **2011**, *6*, 4942.
24. Feng, Q. H.; Li, J. L.; Cheng, H. L.; Chen, F. G.; Xie, Y. M. *Bioresources* **2014**, *9*, 4369.
25. Peñaranda, A. J. E.; Sabino, M. A. *Polym. Bull.* **2010**, *65*, 495.
26. Lora, J. H.; Glasser, W. G. *J. Polym. Environ.* **2002**, *10*, 39.
27. Pye, E. K.; Lora, J. H. *Tappi J.* **1991**, *74*, 113.
28. Pan, X. J.; Kadla, J.; Ehara, K.; Gilkes, N.; Saddler, J. *J. Agric. Food Chem.* **2006**, *54*, 5806.
29. Xue, B. L.; Wen, J. L.; Xu, F.; Sun, R. C. *J. Appl. Polym. Sci.* **2012**, *129*, 434.
30. Yang, J.; Han, C. R.; Duan, J. F.; Ma, M. G.; Zhang, X. M.; Xu, F.; Sun, R. C.; Xie, X. M. *J. Mater. Chem.* **2012**, *22*, 22467.
31. Mallapragada, S. K.; Peppas, N. *J. Appl. Polym. Sci.* **1996**, *34*, 1339.
32. Pourjavadi, A.; Ayyari, M.; Amini-Fazl, M. S. *Eur. Polym. J.* **2008**, *44*, 1209.
33. Tang, Q. W.; Sun, X. M.; Li, Q. H.; Wu, J. H.; Lin, J. M. *Colloids Surf. A: Physicochem. Eng. Aspects* **2009**, *346*, 91.
34. Ye, D. Z.; Jiang, X. C.; Xia, C.; Liu, L.; Zhang, X. *Carbohydr. Polym.* **2012**, *89*, 876.
35. Marandi, G. B.; Esfandiari, K.; Biranvand, F.; Babapour, M.; Sadeh, S.; Mahdavinia, G. R. *J. Appl. Polym. Sci.* **2008**, *109*, 1083.
36. Song, Y.; Zhou, J.; Zhang, L.; Wu, X. *Carbohydr. Polym.* **2008**, *73*, 18.
37. Wu, Y. X.; Zhou, J. H.; Ye, C. C.; Sun, H. Z.; Zhao, R. J. *Iran. Polym. J.* **2010**, *19*, 511.
38. Park, Y. D.; Tirelli, N.; Hubbell, J. A. *Biomaterials* **2003**, *24*, 893.
39. Ciolacu, D.; Oprea, A. M.; Anghel, N.; Cazacu, G.; Cazacu, M. *Mater. Sci. Eng. C* **2012**, *32*, 452.
40. Tuncaboylu, D. C.; Sari, M.; Oppermann, W.; Okay, O. *Macromolecules* **2011**, *44*, 4997.